

non relativistic: Schrödinger

L(S)DA

scalar relativistic

GGA

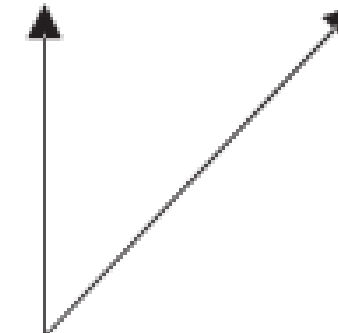
relativistic: Dirac

hybrids

MGGA

Lagrange multipliers
band structure

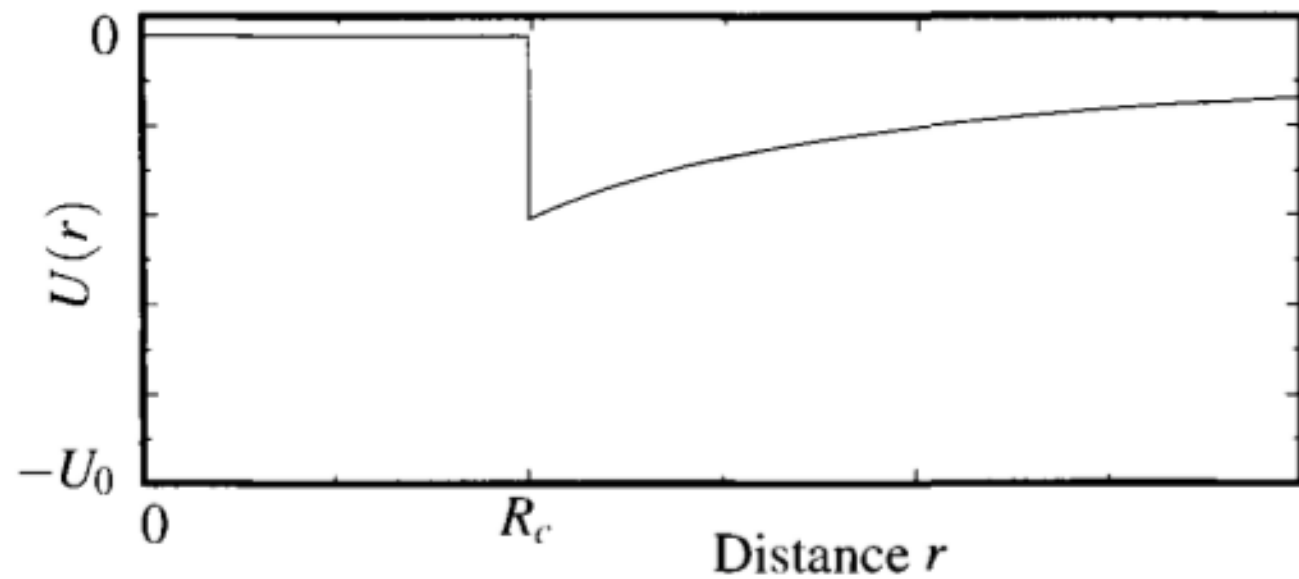
$$\left[-\frac{\nabla^2}{2m} + v_{ext}(\mathbf{r}) + v_H(\mathbf{r}) + v_{xc}(\mathbf{r}) \right] \phi_n(\mathbf{r}) = \varepsilon_n \phi_n(\mathbf{r})$$

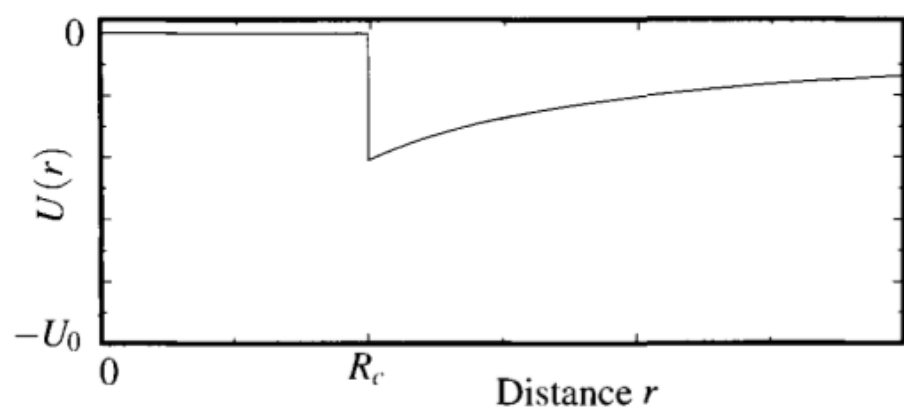
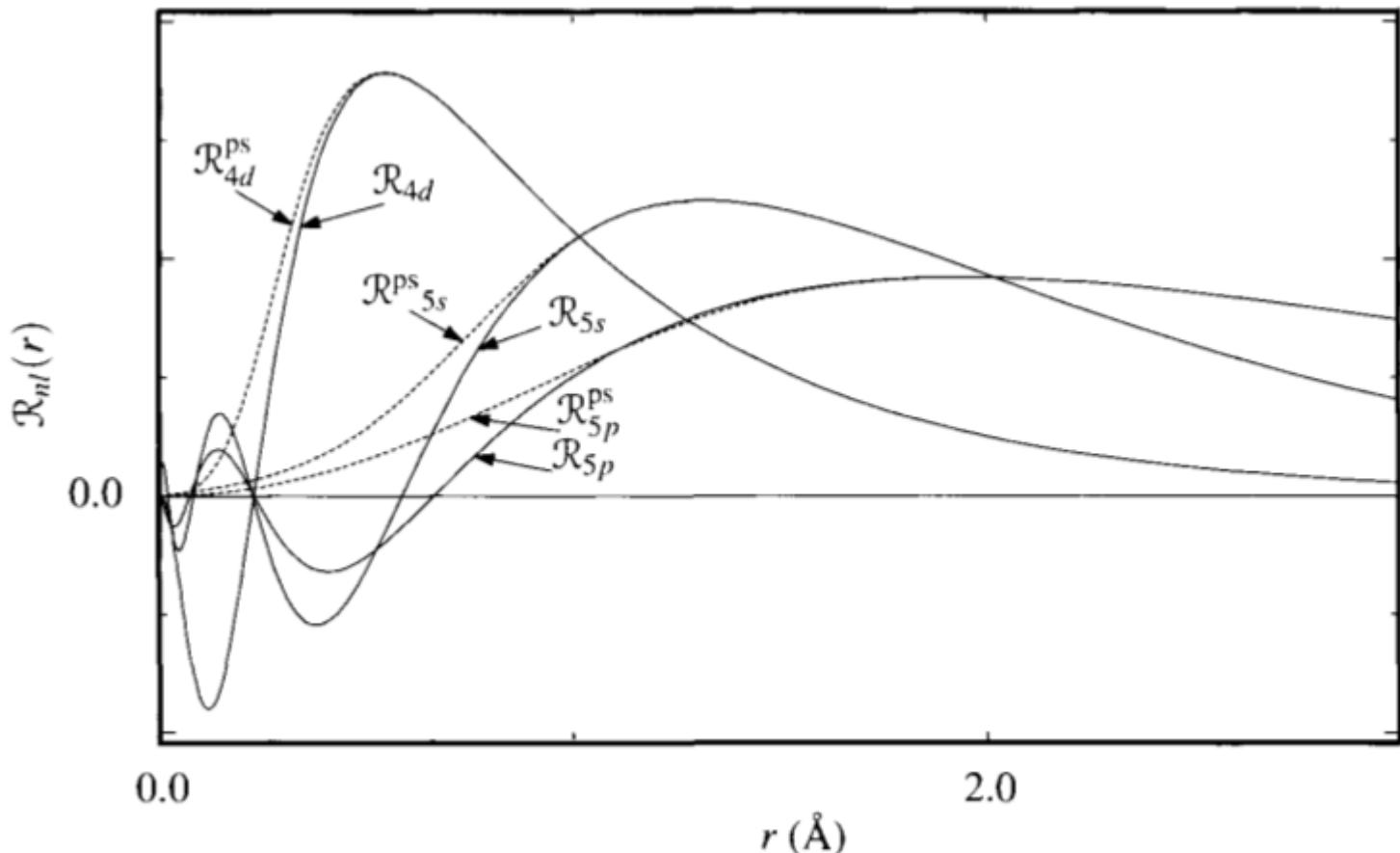


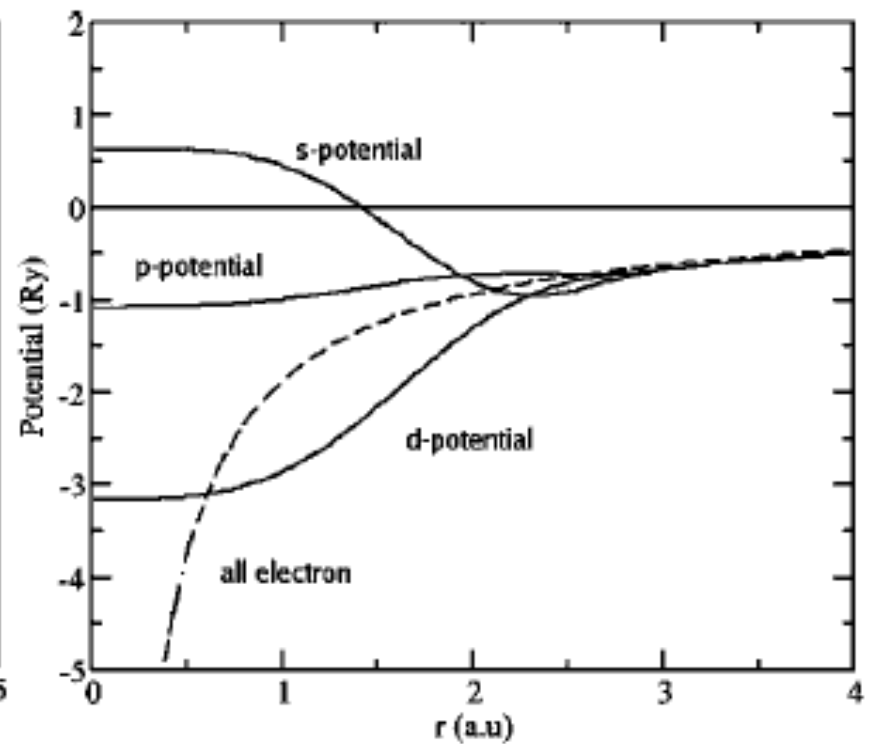
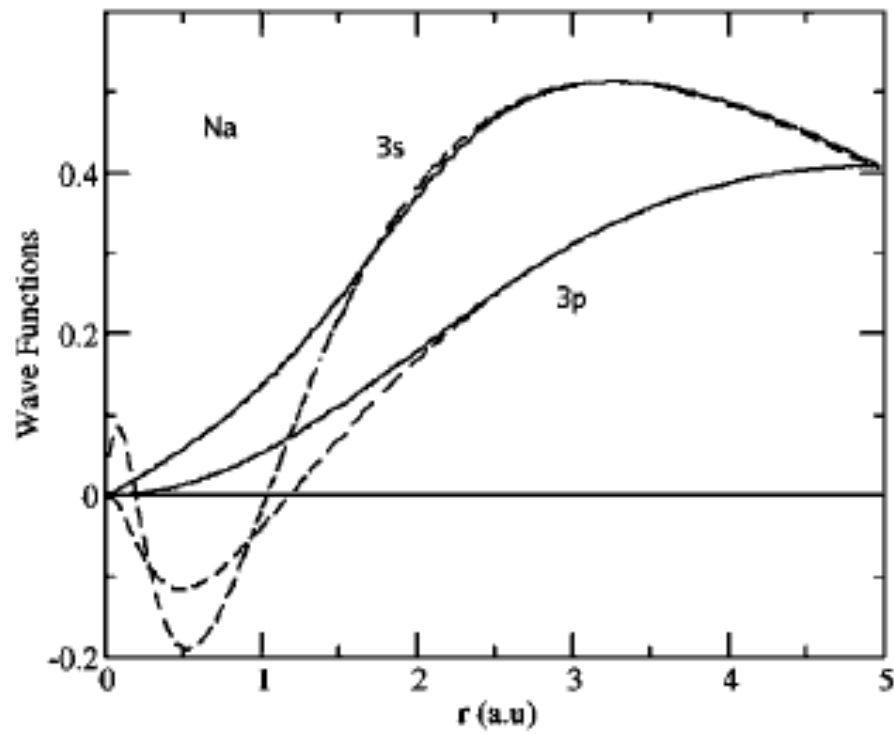
nuclei
pseudopotential

Poisson eq.
integral

mesh/basis
GTO/STO/...
LMTO/LAPW/PW/...

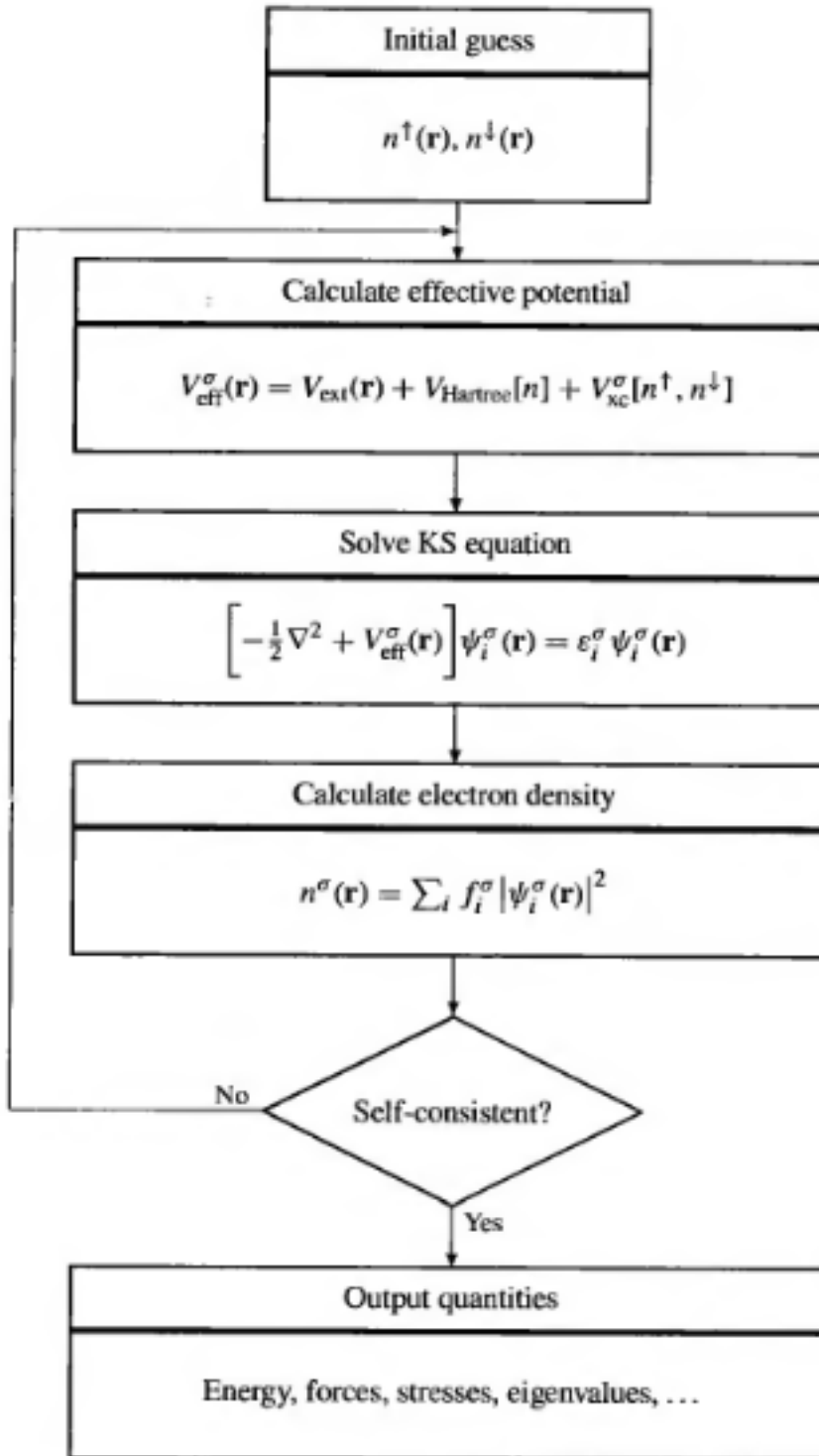


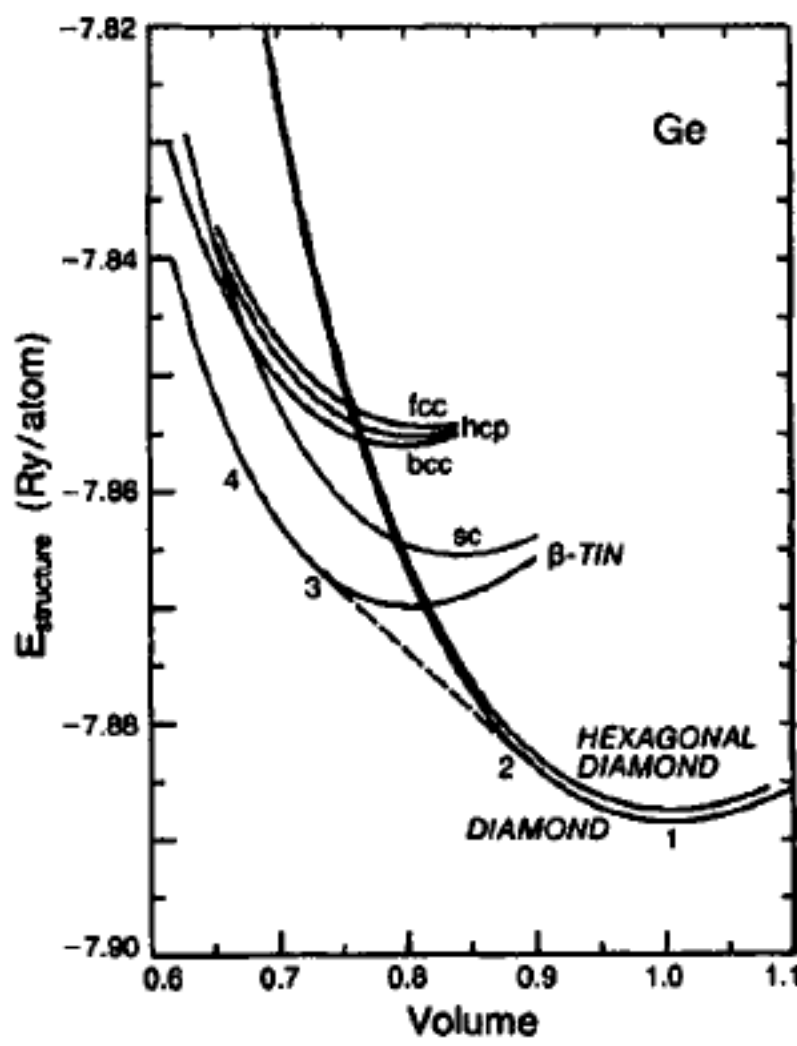
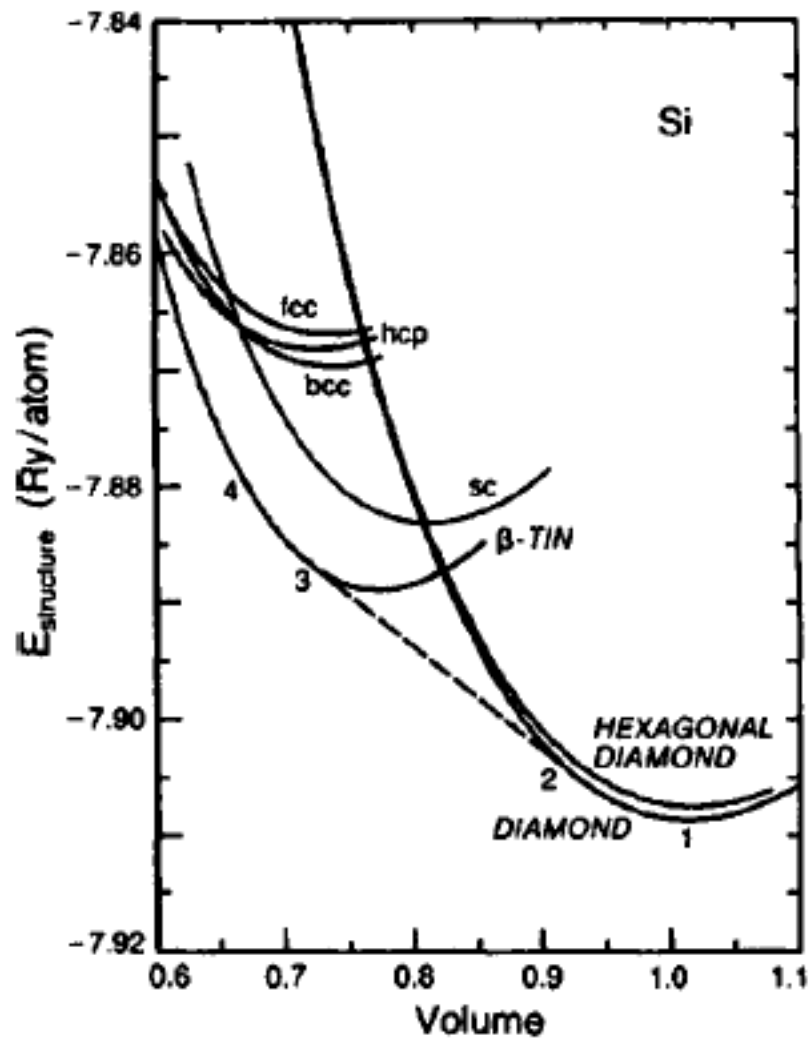




S.G. Louie, em Conceptual Foundations of Materials, Eds. S.G. Louie e M.L. Cohen, Elsevier, 2006.

Self-consistent Kohn–Sham equations





Yin e Cohen, 1982.

Table 2. Comparison of calculated LDA and HF band gaps (in eV) with experiment.

	HF	LDA	Experiment ^a
Diamond	13.6	3.9	5.48
Si	6.4	0.5	1.17
Ge	4.9	-0.26	0.74
LiCl	16.9	6.0	9.4

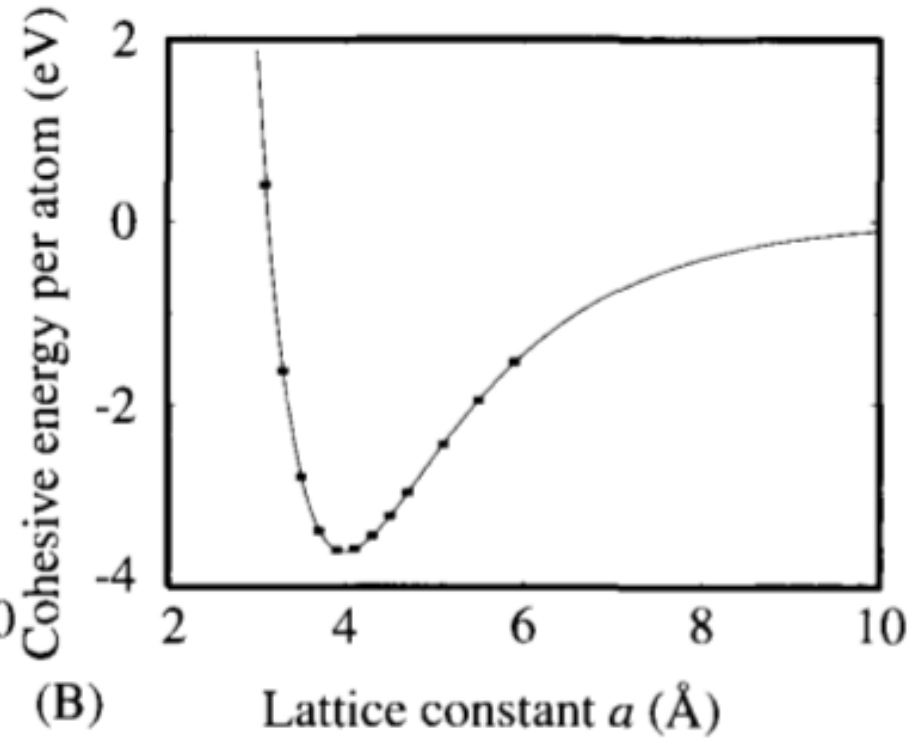
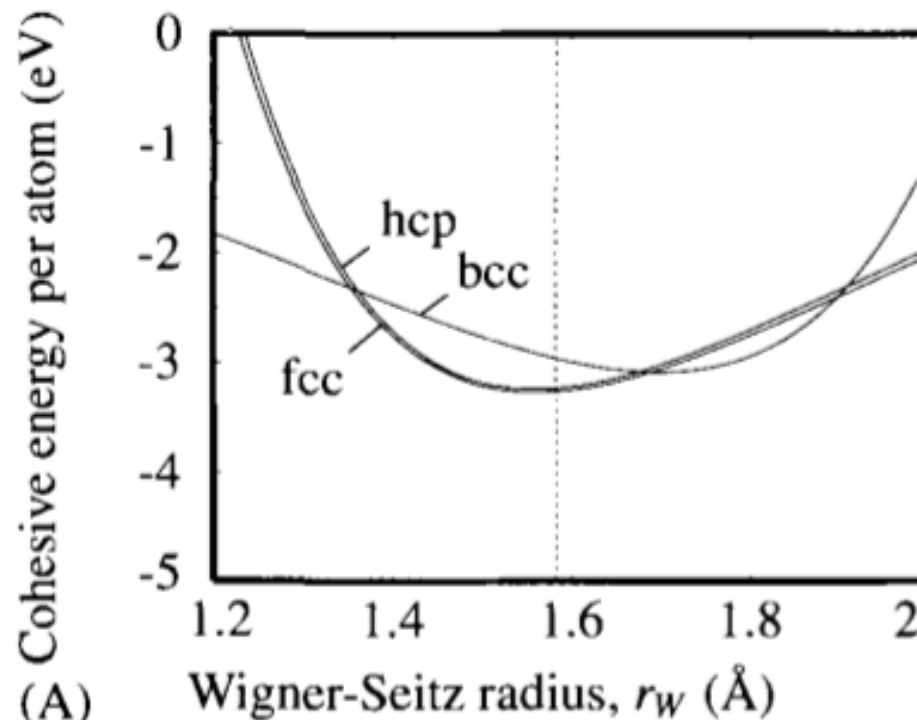
^aSource: Kittel [98].

Table 9.2. Hartree–Fock and LDA compared with experiment

Atom	LDA (KS)	Hartree–Fock	LDA (PZ)	Experiment
He	−2.83	−2.86	−2.92	−2.90
Li	−7.33	−7.43	−7.50	−7.48
Ne	−128.12	−128.55	−129.27	−128.94
Ar	−525.85	−526.82	−528.39	−527.60

Total energies of atoms in Hartrees (27.2107 eV), comparing Hartree–Fock, the local density approximation, LDA (KS) as first described by Kohn and Sham, the local density approximation LDA (PZ) as improved by Perdew and Zunger (1981), and experiment. Source: Tong and Sham (1966) and Perdew and Zunger (1981).

Extraído do Marder.



Tests of a ladder of density functionals for bulk solids and surfaces

Viktor N. Staroverov and Gustavo E. Scuseria

Department of Chemistry, Rice University, Houston, Texas 77005, USA

Jianmin Tao and John P. Perdew

Department of Physics and Quantum Theory Group, Tulane University, New Orleans, Louisiana 70118, USA

(Received 4 September 2003; revised manuscript received 13 November 2003; published 13 February 2004)

The local spin-density approximation (LSDA) and the generalized gradient approximation (GGA) of Perdew, Burke, and Ernzerhof (PBE) are fully non-empirical realizations of the first two rungs of “Jacob’s ladder” of exchange-correlation density functionals. The recently proposed non-empirical meta-GGA of Tao, Perdew, Staroverov, and Scuseria (TPSS), featuring the kinetic energy density as an additional local ingredient, completes the third rung. A hierarchy of these functionals, complemented by the meta-GGA of Perdew, Kurth, Zupan, and Blaha (PKZB), is tested in self-consistent Gaussian-type orbital calculations of equilibrium lattice constants, bulk moduli, and cohesive energies for 18 solids, and in studies of the jellium surface energy. The ascent of the ladder generally results in better performance, although most of the improvement for bulk solids occurs in the transition from LSDA to PBE. For the jellium surface energy, PBE is less accurate than LSDA, but PKZB and TPSS are more accurate. We support the idea that most of the error of these functionals for bulk solids arises in the description of core–valence interaction, by demonstrating that it can be removed through adjustment of the corresponding term in the equation of state. Overall, TPSS gives the best description of solids and surfaces, as it was found to do for molecules in earlier work.

Solid	a_0^{LSDA}	a_0^{PBE}	a_0^{PKZB}	a_0^{TPSS}	Expt.
Li	3.383	3.453	3.512	3.475	3.477(3.451)
Na	4.049	4.199	4.305	4.233	4.225(4.210)
K	5.093	5.308	5.494	5.362	5.225(5.212)
Al	4.008	4.063	4.040	4.035	4.032(4.020)
C	3.544	3.583	3.592	3.583	3.567(3.556)
Si	5.426	5.490	5.475	5.477	5.430(5.423)
SiC	4.351	4.401	4.404	4.392	4.358(4.349)
Ge	5.633	5.765	5.729	5.731	5.652(5.646)
GaAs	5.592	5.726	5.698	5.702	5.648(5.643)
NaCl	5.471	5.698	5.801	5.696	5.595(5.580)
NaF	4.505	4.700	4.764	4.706	4.609(4.594)
LiCl	4.968	5.148	5.220	5.113	5.106(5.090)
LiF	3.904	4.062	4.109	4.026	4.010(3.987)
MgO	4.156	4.242	4.265	4.224	4.207(4.197)
Cu	3.530	3.636	3.616	3.593	3.603(3.596)
Rh	3.791	3.871	3.844	3.846	3.798(3.793)
Pd	3.851	3.950	3.928	3.917	3.881(3.877)
Ag	3.997	4.130	4.101	4.076	4.069(4.064)
m.e. (Å)	-0.069 (-0.058)	0.052 (0.063)	0.078 (0.089)	0.039 (0.050)	...
m.a.e. (Å)	0.069 (0.058)	0.057 (0.064)	0.078 (0.089)	0.040 (0.050)	...
m.a.r.e. (%)	1.55 (1.31)	1.25 (1.40)	1.65 (1.92)	0.83 (1.07)	...

TABLE III. Equilibrium lattice constants (\AA) of the 18 test solids at 0 K calculated from the SJEOS of Eq. (16). The Murnaghan EOS of Eq. (15) yields identical results within the reported number of decimal places. Experimental a_0 values are from Ref. 68 (Li) and Ref. 69 (Na, K, Al, NaCl, NaF, LiCl, LiF, MgO). The rest are based on room temperature values corrected to the $T=0$ limit using linear thermal expansion coefficients from Ref. 70. The numbers in parentheses refer to experimental values with an estimate of the zero-point anharmonic expansion subtracted out. (The calculated values are precise to within 0.001 \AA for the given basis sets, although basis-set incompleteness limits the accuracy to one less digit.)

TABLE IV. Equilibrium bulk moduli (GPa) of the 18 test solids at 0 K calculated from equations of state (15) and (16). The third section lists bulk moduli corrected by Eq. (21). Experimental values, also for 0 K, are from Ref. 74 (Li), Ref. 75 (Na, extrapolated to 0 K), Ref. 76 (K), Ref. 77 (Al), Ref. 78 (C), Ref. 69 (Si, Ge, GaAs), Ref. 79 (SiC, 298 K), Ref. 80 (NaCl, NaF, LiCl), Ref. 81 (LiF), Ref. 82 (MgO), Ref. 83 (Cu), Ref. 84 (Rh), Ref. 85 (Pd), and Ref. 86 (Ag).

Solid	Murnaghan EOS				SJEOS				Corrected SJEOS				Expt.
	B_0^{LSDA}	B_0^{PBE}	B_0^{PKZB}	B_0^{TPSS}	B_0^{LSDA}	B_0^{PBE}	B_0^{PKZB}	B_0^{TPSS}	$\tilde{B}_0^{\text{LSDA}}$	\tilde{B}_0^{PBE}	$\tilde{B}_0^{\text{PKZB}}$	$\tilde{B}_0^{\text{TPSS}}$	
Li	14.7	13.6	13.2	13.2	14.7	13.7	13.2	13.2	13.2	13.3	13.8	13.2	13.0
Na	9.1	7.7	7.4	7.3	9.2	7.8	7.4	7.3	7.3	7.5	8.0	7.4	7.5
K	4.6	3.8	3.5	3.6	4.6	3.8	3.5	3.6	4.0	4.1	4.1	4.2	3.7
Al	81.8	76.2	88.9	84.7	82.5	76.8	89.4	85.2	78.9	81.4	90.6	85.7	79.4
C	454	422	418	417	458	426	422	421	443	436	438	431	443
Si	95.1	88.6	94.6	91.5	95.6	89.0	94.9	91.9	95.1	95.6	99.4	96.8	99.2
SiC	224	207	211	211	225	209	212	213	223	221	225	223	225
Ge	75.7	62.8	67.9	66.2	75.9	63.0	68.1	66.4	73.8	74.3	76.1	74.5	75.8
GaAs	81.1	68.0	71.6	70.0	81.3	68.1	71.8	70.1	75.4	75.3	76.7	75.1	75.6
NaCl	32.2	23.7	21.5	22.9	32.5	23.9	21.6	23.0	27.0	27.7	27.5	26.6	26.6
NaF	62.8	47.3	44.3	43.7	63.3	47.7	44.5	44.0	53.3	54.1	54.6	50.6	51.4
LiCl	41.8	32.7	29.8	34.1	42.0	32.9	30.0	34.3	34.6	34.8	34.7	34.6	35.4
LiF	86.8	65.4	65.0	66.5	87.5	65.9	65.4	67.2	72.4	71.7	76.4	69.1	69.8
MgO	182	161	159	168	183	162	160	169	171	170	172	173	165
Cu	188	150	161	171	192	153	163	173	161	164	167	170	142
Rh	303	239	248	257	309	243	253	262	304	289	284	294	269
Pd	235	177	184	200	240	180	187	203	222	215	211	223	195
Ag	149	106	115	127	153	107	117	129	126	125	126	131	109
m.e. (GPa)	13.1	-7.4	-4.5	-1.7	14.7	-6.3	-3.4	-0.5	5.5	4.1	5.5	5.4	...
m.a.e. (GPa)	13.7	8.4	8.4	8.4	15.1	7.6	7.8	8.2	6.6	6.0	6.2	7.7	...
m.a.r.e. (%)	15.2	7.1	8.0	7.6	16.2	6.8	7.8	7.5	5.1	5.0	6.3	5.9	...

TABLE VI. Cohesive energies (eV/atom) of 8 selected solids at 0 K, corrected for zero-temperature motion effects. Experimental values are based on zero-temperature enthalpies of formation ($\Delta_f H_0^\circ$) of the crystals and gaseous atoms taken from Ref. 88 (Ge) and Ref. 89 (all others).

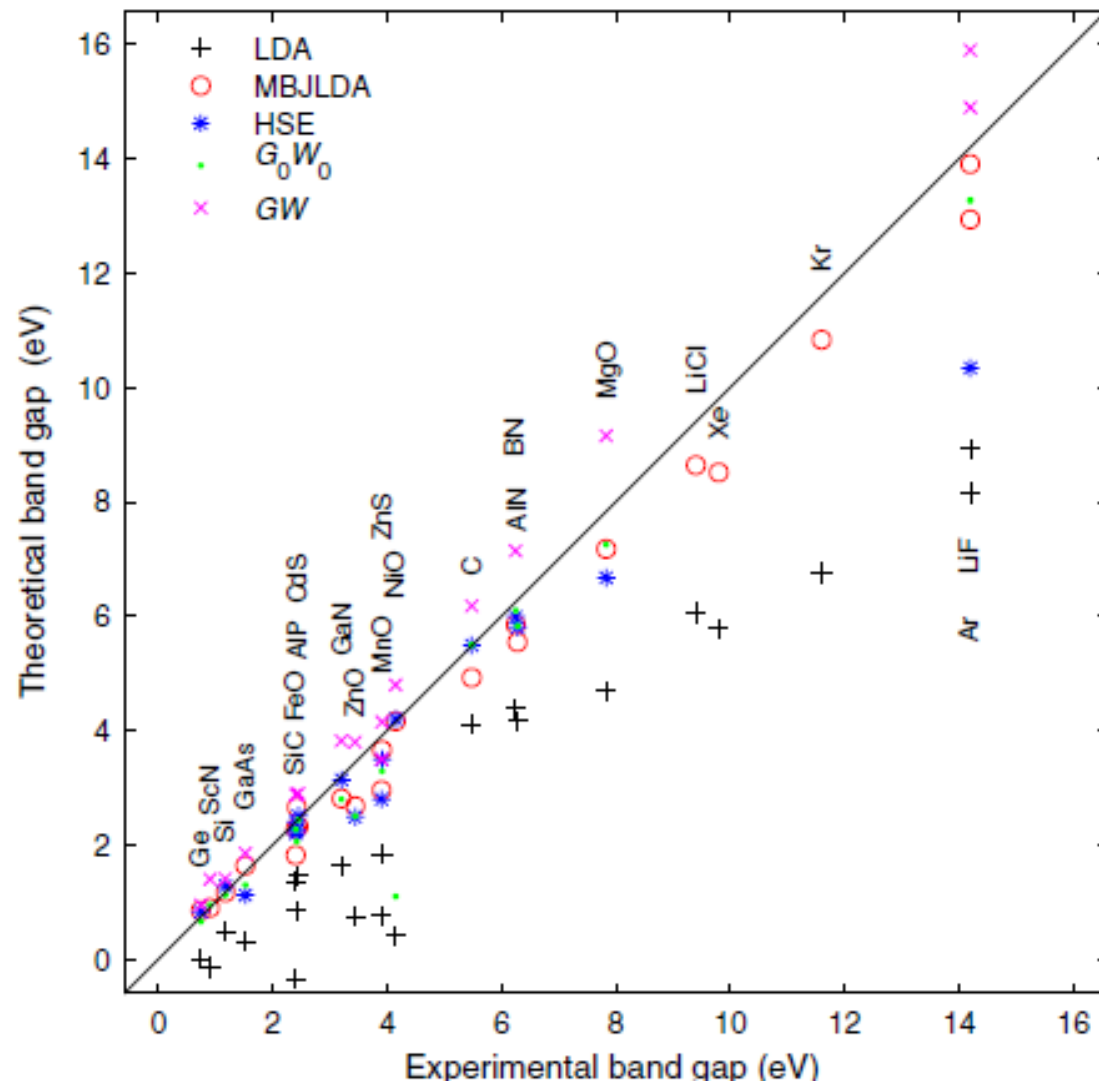
Solid	$\varepsilon_0^{\text{LSDA}}$	$\varepsilon_0^{\text{PBE}}$	$\varepsilon_0^{\text{PKZB}}$	$\varepsilon_0^{\text{TPSS}}$	Expt.
C	8.83	7.62	7.14	7.12	7.37
Si	5.26	4.50	4.39	4.36	4.62
SiC	7.25	6.25	5.98	6.02	6.37
Ge	4.72	3.82	3.58	3.78	3.87
NaCl	3.58	3.16	3.15	3.18	3.31
NaF	4.50	3.96	3.81	3.87	3.93
LiCl	3.88	3.41	3.33	3.41	3.55
LiF	5.02	4.42	4.25	4.32	4.40
m.e. (eV/atom)	0.70	-0.04	-0.22	-0.17	...
m.a.e. (eV/atom)	0.70	0.11	0.22	0.17	...
m.a.r.e. (%)	14.4	2.4	4.9	3.5	...

Accurate Band Gaps of Semiconductors and Insulators with a Semilocal Exchange-Correlation Potential

Fabien Tran and Peter Blaha

Institute of Materials Chemistry, Vienna University of Technology, Getreidemarkt 9/165-TC, A-1060 Vienna, Austria

(Received 5 December 2008; published 3 June 2009)



Solid	LDA	MBJLDA	HSE	G_0W_0	GW	Expt.
Ne (A1)	11.42	22.72		19.59 ^e	22.1 ^g	21.70
Ar (A1)	8.16	13.91	10.34 ^a	13.28 ^e	14.9 ^g	14.20
Kr (A1)	6.76	10.83				11.6
Xe (A1)	5.78	8.52				9.8
C (A4)	4.11	4.93	5.49 ^b	5.50 ^e	6.18 ^g	5.48
Si (A4)	0.47	1.17	1.28 ^b	1.12 ^e	1.41 ^g	1.17
Ge (A4)	0.00	0.85	0.83 ^b	0.66 ^f	0.95 ^g	0.74
LiF (B1)	8.94	12.94		13.27 ^e	15.9 ^g	14.20
LiCl (B1)	6.06	8.64				9.4
MgO (B1)	4.70	7.17	6.67 ^b	7.25 ^e	9.16 ^g	7.83
ScN (B1)	-0.14	0.90		0.95 ^f	1.4 ^h	~0.9
MnO (B1)	0.76	2.95	2.8 ^c		3.5 ⁱ	3.9 ± 0.4
FeO (B1)	-0.35	1.82	2.2 ^c			2.4
NiO (B1)	0.42	4.16	4.2 ^c	1.1 ^f	4.8 ⁱ	4.0, 4.3
SiC (B3)	1.35	2.28	2.40 ^b	2.27 ^e	2.88 ^g	2.40
BN (B3)	4.39	5.85	5.99 ^b	6.10 ^e	7.14 ^g	~6.25
GaN (B3)	1.63	2.81	3.14 ^b	2.80 ^e	3.82 ^g	3.20
GaAs (B3)	0.30	1.64	1.12 ^b	1.30 ^e	1.85 ^g	1.52
AlP (B3)	1.46	2.32	2.51 ^b	2.44 ^e	2.90 ^g	2.45
ZnS (B3)	1.84	3.66	3.49 ^b	3.29 ^e	4.15 ^g	3.91
CdS (B3)	0.86	2.66	2.25 ^b	2.06 ^e	2.87 ^g	2.42
AlN (B4)	4.17	5.55	5.81 ^b	5.83 ^f		6.28
ZnO (B4)	0.75	2.68	2.49 ^d	2.51 ^f	3.8 ^g	3.44



Efficient Band Gap Prediction for Solids

M. K. Y. Chan¹ and G. Ceder²

¹*Physics/Materials Science and Engineering, Massachusetts Institute of Technology, Cambridge, Massachusetts 02139, USA*

²*Materials Science and Engineering, Massachusetts Institute of Technology, Cambridge, Massachusetts 02139, USA*

(Received 27 March 2010; published 5 November 2010)

An efficient method for the prediction of fundamental band gaps in solids using density functional theory (DFT) is proposed. Generalizing the Delta self-consistent-field (Δ SCF) method to infinite solids, the Δ -sol method is based on total-energy differences and derived from dielectric screening properties of electrons. Using local and semilocal exchange-correlation functionals (local density and generalized gradient approximations), we demonstrate a 70% reduction of mean absolute errors compared to Kohn-Sham gaps on over 100 compounds with experimental gaps of 0.5–4 eV, at computational costs similar to typical DFT calculations.

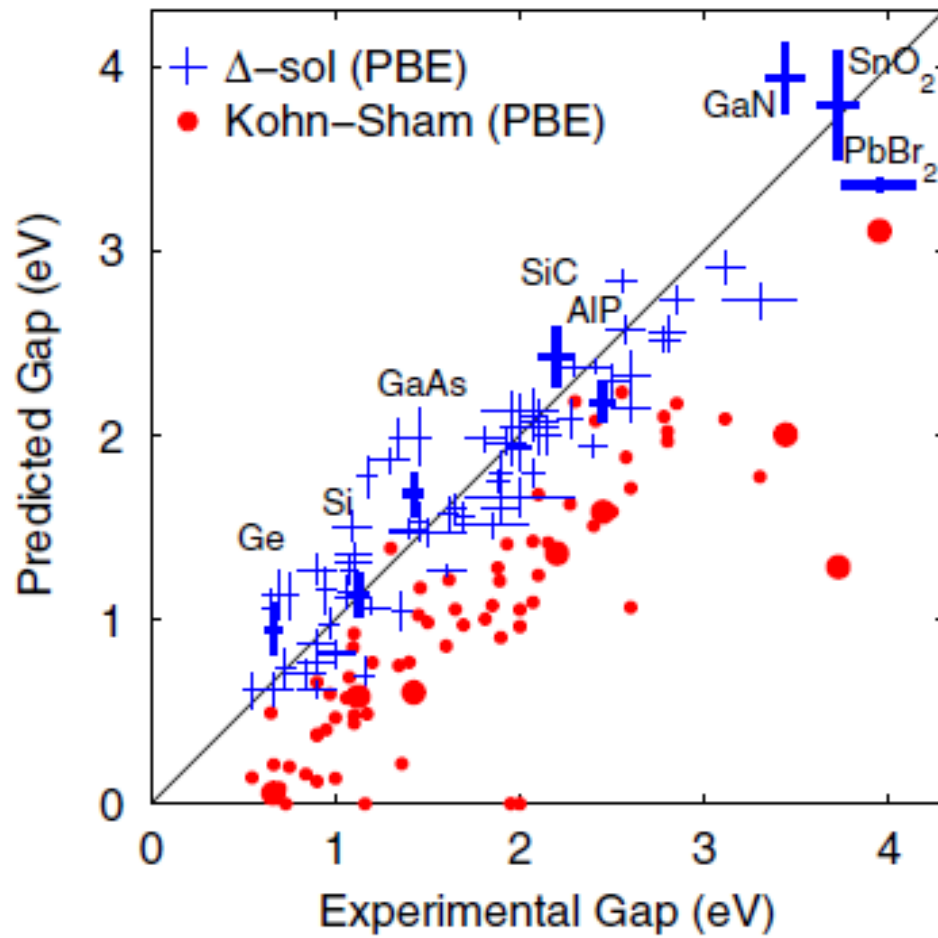
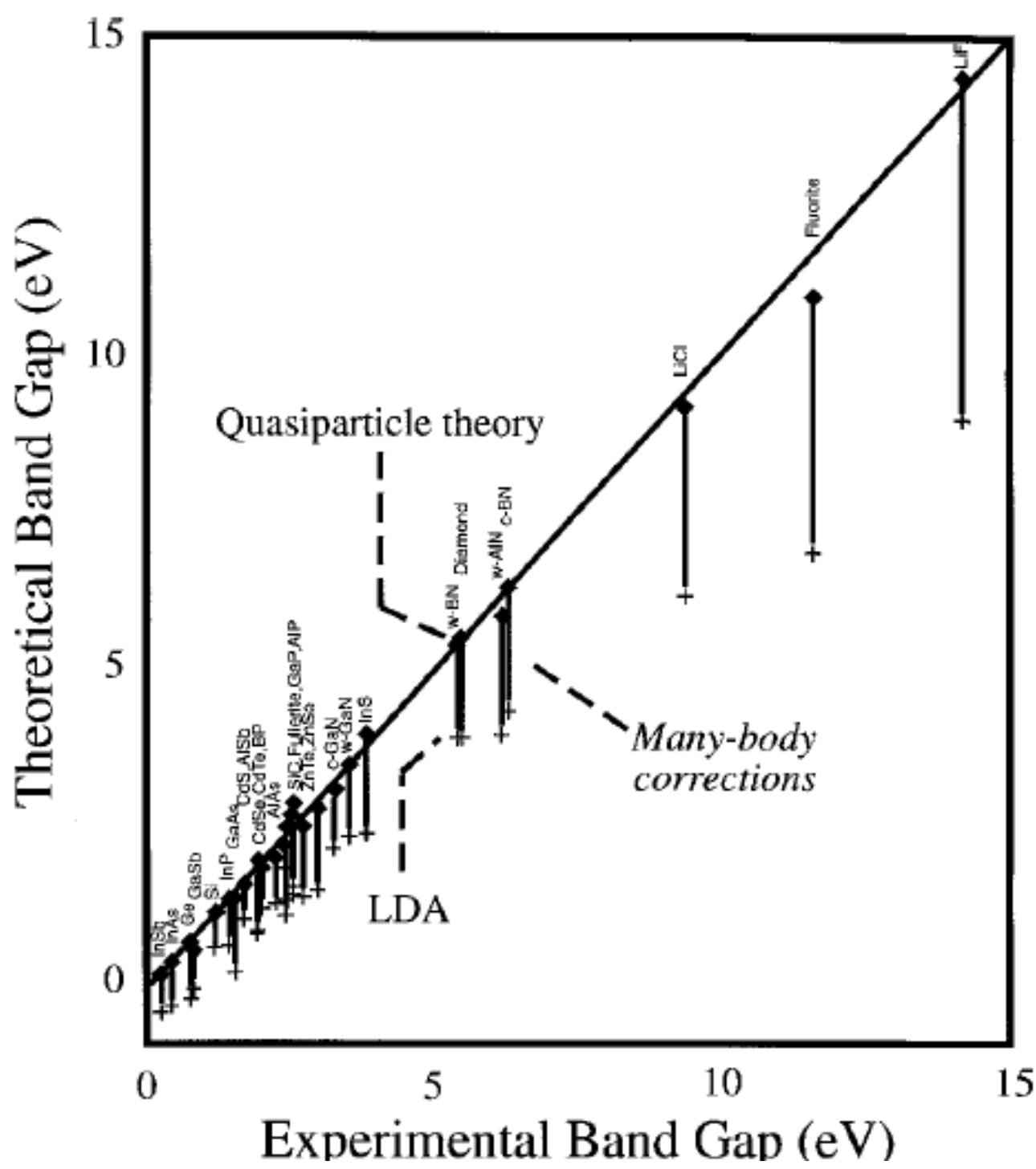
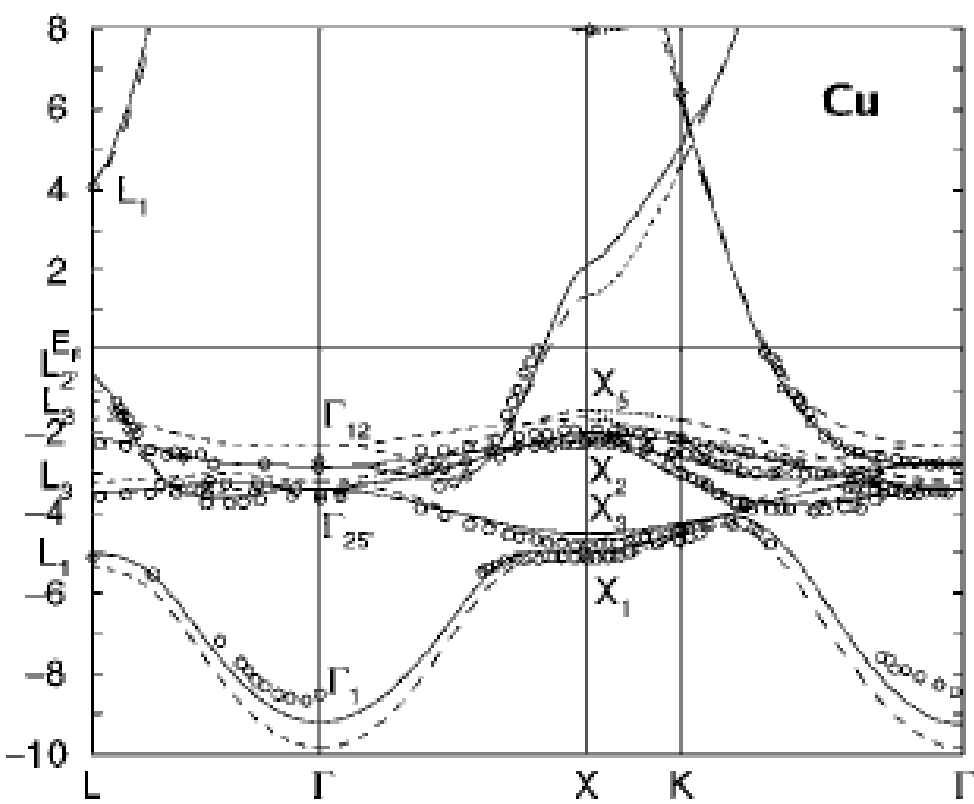
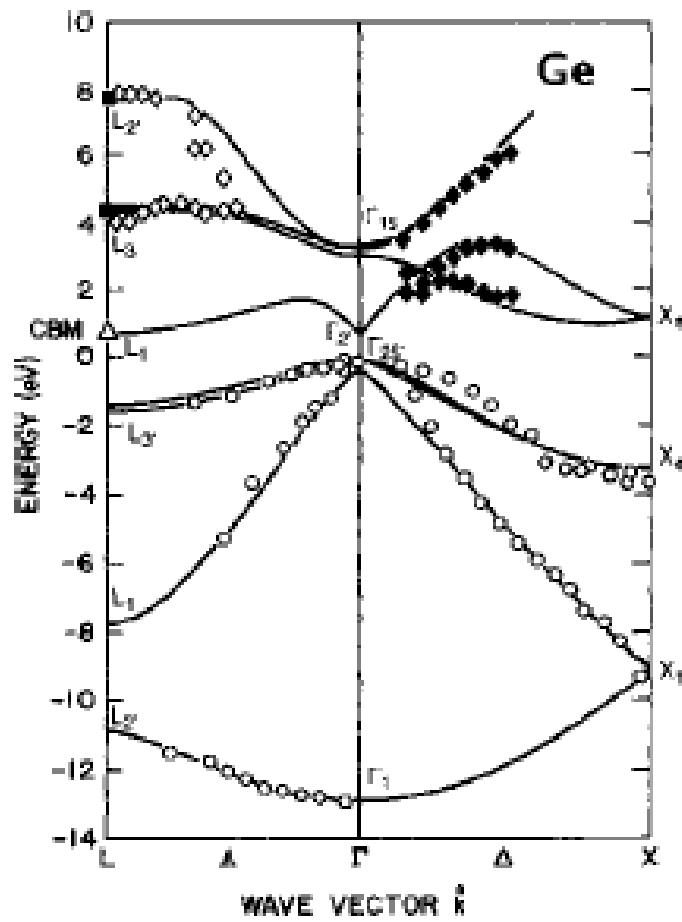


TABLE II. Comparison of Kohn-Sham (KS), MBJ-Kohn-Sham [13], and Δ -sol gaps for LDA. All figures are in eV.

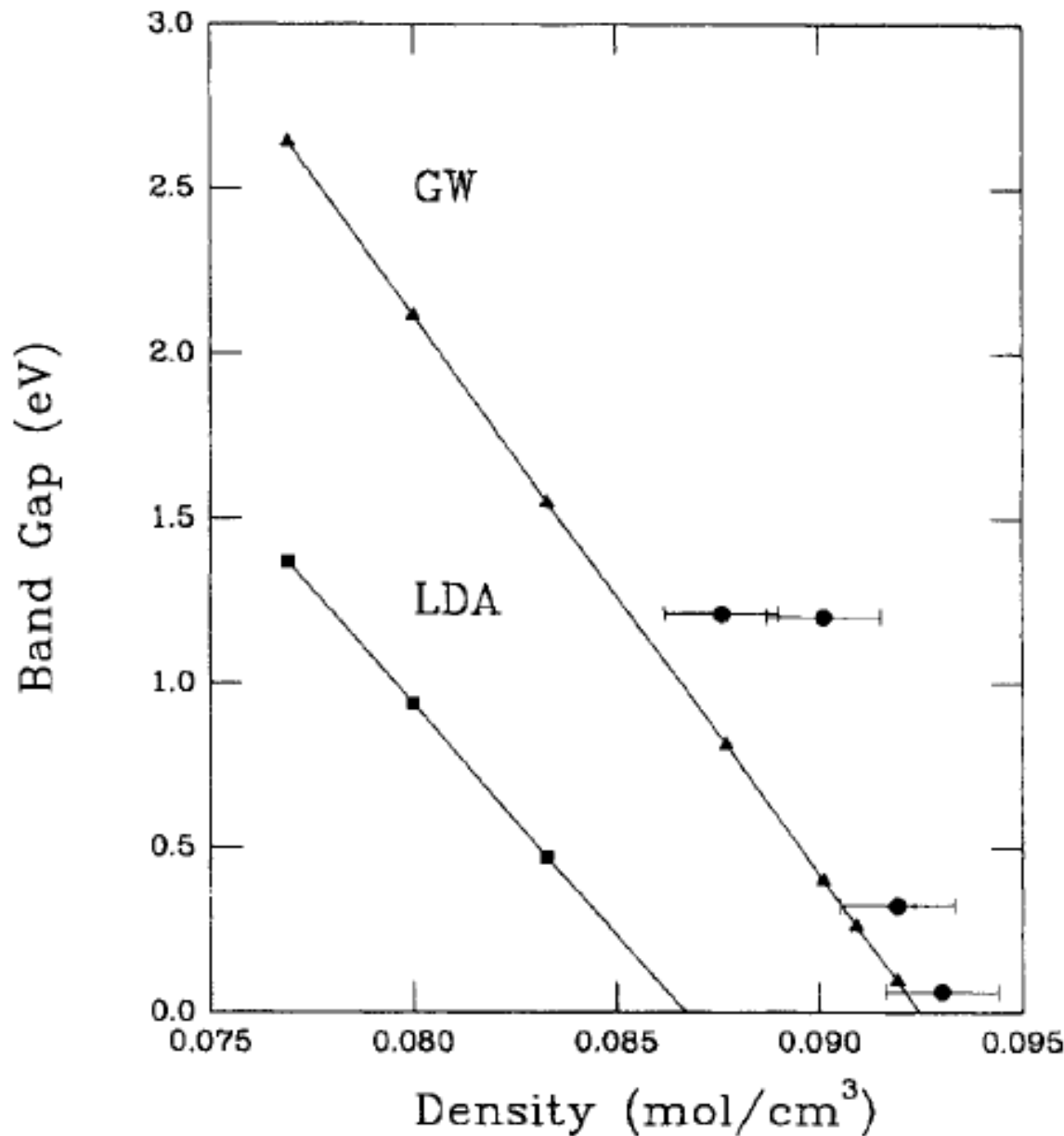
Compound	E_{Exp}	KS_{LDA}	$\text{MBJ-KS}_{\text{LDA}}$	$\Delta\text{-sol}_{\text{LDA}}$
C	5.5	4.1	4.9	5.3
Si	1.1	0.5	1.2	1.0
Ge	0.7	0.0	0.9	0.9
SiC	2.2	1.4	2.3	2.4
BN (cubic)	6.2	4.4	5.9	5.8
GaN	3.4	1.6	2.8	3.9
GaAs	1.4	0.3	1.6	1.5
AlP	2.5	1.5	2.3	2.1
ZnS	3.7	1.8	3.7	3.6
CdS	2.5	0.9	2.7	3.0
AlN	6.1	4.2	5.6	5.3
ZnO	3.3	0.8	2.7	3.5



S.G. Louie, em Conceptual Foundations of Materials, Eds. S.G. Louie e M.L. Cohen, Elsevier, 2006.



S.G. Louie, em Conceptual Foundations of Materials, Eds. S.G. Louie e M.L. Cohen, Elsevier, 2006.



Xe – Chaham et al.,

S.G. Louie, em Conceptual Foundations of Materials, Eds. S.G. Louie e M.L. Cohen, Elsevier, 2006.